JOURNAL OF AIRCRAFT
Vol. 41, No. 2, March–April 2004

Study of Reduced-Order Models for Gust–Response Analysis of Flexible Wings

M. Gennaretti*
Università degli Studi Roma Tre, 00146 Rome, Italy
and
F. Mastroddi†
Università degli Studi di Roma "La Sapienza," 00184 Rome, Italy

Three types of aeroelastic reduced-order models (ROMs) for flutter and gust-response analyses are examined, one of which is introduced here. One is based on the finite-state description of unsteady aerodynamics obtained through a rational-matrix approximation of the frequency-domain transcendental aerodynamic operator. Coupling this with the equations of the structural dynamics yields the aeroelastic ROM. The drawback of this approach is that some aerodynamic states have to be added to the structural states in the state-space format description of the aeroelastic system. The second model that is discussed yields directly the finite-state description of the aeroelastic operator without altering the dimensions of the state space. This model is iterative in nature, in that it requires an estimate of aeroelastic eigenvalues and eigenvectors from the original eigenproblem. Finally, an alternate ROM formulation for the gust-response problem is proposed. It combines good level of accuracy with reduction of additional aerodynamic states and thus can be conveniently used in preliminary design process and control-law synthesis.

Introduction

WITH the exception of the solutions obtained by the elementary quasi-steady aerodynamic models, a linear unsteady-aerodynamics operator relating elastic displacements to aerodynamic forces is of transcendental type in the Laplace domain. This is caused both by the time delays in disturbance propagation induced by flow compressibility and by the memory effects stored in the convected wake vorticity. One of the consequences is that the stability analysis of the aeroelastic model obtained by combining the structural and aerodynamic operators cannot be performed through a standard eigenanalysis because of the transcendental nature of the resulting characteristic equation. Furthermore, when an aerodynamic operator of this type is employed it is not possible to formulate the problem in terms of a time-domain state-space format (unless an infinite-dimension state space is used). To overcome these difficulties, the aerodynamic operator can be approximated by rational expressions involving a finite number of poles that, when transformed into the time domain, provide a description of the aerodynamic forces in terms of a finite number of state variables. Thus, this approximate rational-matrix aerodynamics (RMA) modeling can be conceived in the general frame of reduced-order models[1] (ROMs) for aeroelastic systems.

The numerical simulation obtained by direct step-by-step integration of the coupled equations of structural dynamics and unsteady aerodynamics is computationally expensive. Also the model itself is extremely complex. These facts render this approach useless for preliminary design and active control applications. Indeed, combining structural equations with an aerodynamic ROM, it is possible to yield a simple mathematical description of the system that is suitable for multidisciplinary preliminary design purposes and, at the same time, is capable of predicting the dynamic behavior with a high level of accuracy. In particular, considering a linear unsteady aerodynamic model, the use of finite-state models yields a standard eigenproblem for the aeroelastic stability analysis and a time-domain state-space format representation of the system that is convenient in optimization procedures and control-law synthesis (see Refs. 2–8 for the pioneering formulations and Refs. 9–15 for more recent developments).

ROMs have also been developed for nonlinear unsteady aerodynamics. Most of them are identified through the application of the Volterra theory based on unsteady aerodynamic impulse responses provided by computational-fluid-dynamics solvers,[16–20] but examples of ROMs obtained through the proper orthogonal decomposition (POD) are available (for instance, see Ref. 21 where the Karhunen–Loève decomposition is applied for identification of space-discretized unsteady transonic aerodynamic operators and Ref. 22 where a review of POD activity is given).

A different procedure for obtaining the space-state format description of a linear wing aeroelastic system can be obtained by applying the procedure defined by the p–transform method introduced in Ref. 23. It consists of a finite-state approximation directly applied to the space-discretized aeroelastic operator that yields a constant-coefficient linear system for the structural states in the frequency domain, thereby providing also a time-domain state-space format for the aeroelastic system without introduction of additional variables. For given flight conditions this approach is based on the knowledge of the subset of aeroelastic eigenvalues that are closest to the structural ones, together with the corresponding eigenvectors (evaluated through an iterative eigenprocedure like, e.g., the modified $p-k$ method[24]). A relevant issue that distinguishes the latter approach from that based on the RMA is the accuracy of the two formulations. Indeed, as it will be shown later, when frequency-domain aerodynamic data are available the RMA approach provides approximations of the aerodynamic (and aeroelastic) operator over the complex plane that are as accurate as those along the imaginary axis. On the other hand, the p–transform method (based on the $p-k$ method) yields an approximate aeroelastic operator that is affected by inaccuracies, depending on the distance between the aeroelastic eigenvalues and the imaginary axis (see also Ref. 25 where an approach alternative to the $p-k$ method is outlined).

In the present paper, in addition to the statement of the linear aeroelastic problem of a fixed wing subject to a gust, the p–transform

Received 6 June 2002; revision received 1 June 2003; accepted for publication 16 June 2003. Copyright © 2003 by the American Institute of Aeronautics and Astronautics, Inc. All rights reserved. Copies of this paper may be made for personal or internal use, on condition that the copier pay the $10.00 per-copy fee to the Copyright Clearance Center, Inc., 222 Rosewood Drive, Danvers, MA 01923; include the code 0021-8669/04 $10.00 in correspondence with the CCC.

*Associate Professor, Dipartimento di Ingegneria Meccanica e Industriale, via della Vasca Navale, 79; m.gennaretti@uniroma3.it.

†Associate Professor, Dipartimento di Ingegneria Aerospaziale e Astronautica, via Eudossiana, 16; franco.mastroddi@uniroma1.it.

method and an aeroelastic ROM based on a RMA model will be outlined and compared to assess the difference in accuracy in flutter and gust-response analyses. The availability of a reliable aeroelastic ROM requiring no additional states would be convenient for optimal design applications where a small number of state varables to deal with is desirable, but even more for control-law synthesis purposes. Indeed, the additional states arising in RMA-based aeroelastic models are related to the convected wake vorticity and flow compressibility and thus are not accessible to measurement. Therefore, the definition of control feedback requires the introduction of an observer for the estimation of the additional aerodynamic states, and this, increasing the complexity of the mathematical model to deal with, might considerably decrease the effectiveness of the control procedure.

Among the RMA models currently available, we will apply that presented in Ref. 12, which has been validated by the authors and their coworkers both for fixed[14] and rotary wings.[15] This approach is closely related to the well-known Karpel's method[6,9]; the difference is in some mathematical items for which the a priori choice of number of additional states in Karpel's method is replaced by a self-fitting procedure in that used here (see later and Ref. 12 for a discussion on the relationship between the two formulations).

Finally, starting from the results obtained by the p–transform method and the RMA-based aeroelastic ROM considered, we will propose a novel ROM for gust-response analysis, which mantains the same level of accuracy as the RMA-based approach, while reducing the number of additional states to be introduced. Thus, this could be considered as an alternate ROM that can be conveniently used in preliminary design and synthesis of control law for gust-load alleviation.

Numerical applications will concern flutter and gust-response analyses of two different wing configurations, based on finite element method descriptions for the structures.

Linear Aeroelasticity: Statement of the Problem

Consider an aeroelastic wing system in cruise flight, with elastic deformation described by the Lagrangian coordinates corresponding to the amplitudes $q_j(t)$ $(j = 1, \ldots, M_m)$ of the first M_m natural modes of vibration (here assumed to be normalized, so as to have unit generalized masses). Introducing the nondimensional time $\tau = tV/b$, where V is the air velocity and b is the reference semichord, neglecting structural damping, and collecting all q_j in the M_m-dimensional vector $\boldsymbol{q}$, the dynamics of the system are governed by

$$\frac{\mathrm{d}^2\boldsymbol{q}}{\mathrm{d}\tau^2} + \boldsymbol{\Omega}^2\boldsymbol{q} = q_D\boldsymbol{f}_A \tag{1}$$

that, after Laplace-transformation, becomes, for homogeneous initial conditions,

$$(p^2\boldsymbol{I} + \boldsymbol{\Omega}^2)\tilde{\boldsymbol{q}} = q_D\tilde{\boldsymbol{f}}_A \tag{2}$$

with ˜ denoting Laplace transformation.

In Eq. (2) p is the complex reduced frequency defined as $p = sV/b$ for s denoting the dimensional Laplace variable, and $q_D = \rho V^2/2$ is the dynamic pressure of the unperturbed flow with ρ denoting the air density. In addition, $\boldsymbol{f}_A = \boldsymbol{f}_q + \boldsymbol{f}_g$ is the vector of the generalized aerodynamic forces induced by wing deformation, $\boldsymbol{f}_q$, and gust disturbance, $\boldsymbol{f}_g$, if present, whereas $\boldsymbol{\Omega}^2$ is the diagonal structural nondimensional eigenvalue matrix. In standard fixed-wing aeroelastic analysis one typically assumes linear dependence of $\boldsymbol{f}_A$ both upon the Lagrangean coordinates, q_j, and upon the gust velocity, w_g, therefore limited to potential, fixed-wake, subsonic or supersonic flow cases (i.e., viscous effects and transonic effects are neglected). Then, in the nondimensional Laplace domain the generalized aerodynamic forces caused by wing deformation and gust velocity can be expressed as

$$\tilde{\boldsymbol{f}}_q(p) = \boldsymbol{Q}(p, M)\tilde{\boldsymbol{q}}(p) \tag{3}$$

and

$$\tilde{\boldsymbol{f}}_g(p) = \boldsymbol{g}(p, M)\tilde{w}_g(p) \tag{4}$$

where $\boldsymbol{Q}$ is the aerodynamic matrix, that is, the collection of transfer functions relating generalized aerodynamic forces to structural Lagrangean coordinates, whereas $\boldsymbol{g}$ is the gust aerodynamic (column) matrix, that is, the collection of transfer functions relating generalized aerodynamic forces to the gust-velocity function. The matrices $\boldsymbol{Q}$ and $\boldsymbol{g}$ depend on the flight Mach number, M, and are transcendental functions of the complex reduced frequency, p, because of the time-delay terms arising in the aerodynamic solution from wake-vorticity convection and compressibility of the flow. They are usually evaluated numerically (e.g., by doublet-lattice methods[26]) along the imaginary axis of the p plane, and then $\boldsymbol{Q}(p)$ and $\boldsymbol{g}(p)$ can be obtained by analytic continuation over the Laplace plane.

Combining Eq. (2) with the expressions of forces given in Eqs. (3) and (4) and introducing the vector $\tilde{\boldsymbol{y}}^T = \{\tilde{\boldsymbol{q}}^T \quad p\tilde{\boldsymbol{q}}^T\}$ yield the following form of the aeroelastic system

$$[p\boldsymbol{I} - \boldsymbol{A}(p)]\,\tilde{\boldsymbol{y}} = \boldsymbol{b}(p)\tilde{w}_g$$

(dependence on M is omitted for compactness of notation), where

$$\boldsymbol{A}(p) = \begin{bmatrix} \boldsymbol{0} & \boldsymbol{I} \\ -\boldsymbol{\Omega}^2 + q_D\boldsymbol{Q}(p) & \boldsymbol{0} \end{bmatrix} \tag{5}$$

and

$$\boldsymbol{b}(p) = \begin{Bmatrix} \boldsymbol{0} \\ q_D\boldsymbol{g}(p) \end{Bmatrix}$$

Thus, the following gust-transfer-function matrix relates the $2M_m$ structural states to the gust velocity

$$\boldsymbol{H}(p) = [p\boldsymbol{I} - \boldsymbol{A}(p)]^{-1}\boldsymbol{b}(p) \tag{6}$$

and the transcendental dependence on p of the matrix $\boldsymbol{A}$ (through $\boldsymbol{Q}$) implies that the poles of the aeroelastic system cannot be evaluated solving a standard eigenproblem because they are the roots of the following characteristic equation:

$$|p\boldsymbol{I} - \boldsymbol{A}(p)| = 0 \tag{7}$$

As indicated in the Introduction, three techniques for transforming the transcendental gust-response problem into a convenient rational polynomial-transfer-function problem are outlined in the remainder of the paper. This implies the replacement of Eq. (7) with a standard eigenproblem and the time-domain state-space format representation of the gust-response problem (useful for preliminary design and control purposes).

Aeroelastic ROM from the p–Transform Method

The essential feature of the p–transform method[23] is the identification of an aeroelastic ROM expressed in terms of the structural state variables, with frequency-independent matrix coefficients. This is achieved through a formulation that is based on the results of the aeroelastic spectral analysis performed by the $p-k$ method[27,28] or modified versions of it. For instance, for a given Mach number and for $p = g + ik$ the modified $p-k$ method of Ref. 24 proposes the following approximated expression for the aerodynamic matrix (see later for a discussion about the mathematical meaning of such approximation)

$$\boldsymbol{Q}(p) \approx \boldsymbol{Q}_R(ik) + [\boldsymbol{Q}_I(ik)/k]p \tag{8}$$

where $\boldsymbol{Q}_R$ and $\boldsymbol{Q}_I$ are, respectively, real and imaginary part of $\boldsymbol{Q}$, and the reduced frequency, k, is defined as $k = \omega b/V$, with ω denoting dimensional frequency. Then, using Eq. (8), for the system matrix $\boldsymbol{A}(p)$ we have the new approximated expression [see Eq. (5)]

$$\boldsymbol{A}(p) \approx \boldsymbol{A}_{p-k}(ik) = \begin{bmatrix} \boldsymbol{0} & \boldsymbol{I} \\ -\boldsymbol{\Omega}^2 + q_D\boldsymbol{Q}_R(ik) & \dfrac{q_D\boldsymbol{Q}_I(ik)}{k} \end{bmatrix}$$

where the dependence on the complex reduced frequency, p, has been replaced by that on the reduced frequency, k. The corresponding stability eigenproblem is expressed in the following form:

$$[p_m \boldsymbol{I} - \boldsymbol{A}_{p-k}(ik_m)]\, \boldsymbol{z}^{(m)} = 0 \tag{9}$$

from which the approximate aeroelastic eigenvalues, p_m, and right eigenvectors, $\boldsymbol{z}^{(m)}$, can be iteratively evaluated (for k_m equal to the imaginary part of p_m) following the $p-k$ procedure.[24]

The core of the p–transform method consists of a two-step procedure.[23] First, $2M_m$ aeroelastic eigenproblems like that in Eq. (9) are solved iteratively, each iterative process starting from one of the $2M_m$ structural eigenvalues. Next, matrix $\boldsymbol{A}$ (for fixed ρ, M, V) is approximated by the following spectral decomposition

$$\boldsymbol{A}(p) \approx \bar{\boldsymbol{A}} = \boldsymbol{Z} \begin{bmatrix} \ddots & & \\ & p_m & \\ & & \ddots \end{bmatrix} \boldsymbol{Y} \tag{10}$$

where $\boldsymbol{Z}$ is the matrix that collects the right aeroelastic eigenvectors $\boldsymbol{z}^{(m)}$ as columns, whereas $\boldsymbol{Y} = \boldsymbol{Z}^{-1}$. (The rows of $\boldsymbol{Y}$ coincide with the normalized left eigenvectors of $\bar{\boldsymbol{A}}$.)

Note the following:

1) Because of the approximations in Eq. (8), among the $2M_m$ eigenvalues p_m, only those placed on the imaginary axis (if they exist) are exact aeroelastic poles [i.e., satisfy Eq. (7)].

2) By construction, the standard spectral analysis performed on matrix $\bar{\boldsymbol{A}}$ gives exactly the same eigenvalues and right eigenvectors calculated by the $p-k$ method.

3) The left eigenvectors of $\bar{\boldsymbol{A}}$ do not coincide with the left eigenvectors of $\boldsymbol{A}_{p-k}(ik_m)$ corresponding to the eigenvalues p_m [see Eq. (9)].

Dykman and Rodden[23] discuss also the modeling of the gust-response problem. They approximate the gust-force vector $\boldsymbol{b}$ by a p-independent constant vector $\bar{\boldsymbol{b}}$ in the following way:

$$\boldsymbol{b}(p) \approx \bar{\boldsymbol{b}} = \sum_{m}^{2M_m} \hat{b}_m \boldsymbol{z}^{(m)} \tag{11}$$

with

$$\hat{b}_m = \boldsymbol{b}^T(ik_m)\hat{\boldsymbol{y}}^{(m)} \tag{12}$$

where $\boldsymbol{b}(ik_m)$ denotes the gust-force vector evaluated at the reduced frequency corresponding to the imaginary part of the eigenvalue p_m, whereas $\hat{\boldsymbol{y}}^{(m)}$ is the left eigenvector of $\boldsymbol{A}_{p-k}(ik_m)$ corresponding to the same eigenvalue. The combination of Eq. (6) with Eqs. (10) and (11) yields the following approximate gust-transfer-function matrix[23]

$$\boldsymbol{H}_{p-t}(p) = [p\boldsymbol{I} - \bar{\boldsymbol{A}}]^{-1}\bar{\boldsymbol{b}}$$

which relates gust velocity to the $2M_m$ structural states.

Analysis of the Gust-Force Vector Approximation

As already observed, if p_m and $\boldsymbol{z}^{(m)}$ are eigenvalue and right eigenvector of $\boldsymbol{A}_{p-k}(ik_m)$ obtained through the $p-k$ method by definition they are also eigenvalue and right eigenvector of $\bar{\boldsymbol{A}}$, but the corresponding left eigenvectors are different. Indeed, following the $p-k$ procedure, one solves (iteratively) $2M_m$ eigenproblems, each solution concerning a matrix $\boldsymbol{A}_{p-k}$ evaluated at different points of the imaginary axis, and yielding one of the aeroelastic eigenvalues p_m and one of the aeroelastic right eigenvectors $\boldsymbol{z}^{(m)}$. Each of these eigenproblems gives a set of $2M_m$ eigenvalues and a set of $2M_m$ right eigenvectors (including the aeroelastic ones), as well as a set of $2M_m$ left eigenvectors, which can be considered as an approximation of the spectral decomposition of the aeroelastic system in the neighborhood of the imaginary part of the corresponding aeroelastic eigenvalue. On the other hand, the p–transform method defines a novel spectral decomposition for the aeroelastic system collecting the solutions of the $2M_m$ eigenproblems examined [see Eq. (10)] and extending their meaning over the whole complex plane, although each solution is valid only at a specified point of the imaginary axis. This spectral decomposition yields the same eigenvalues as those determined by the $p-k$ method, but provides sets of p-independent right and left eigenvectors, which can be considered as average eigenvector bases for the aeroelastic system (not locally accurate in the p plane).

From these observations it follows that the approximation of the gust-force vector suggested in Ref. 23, which consists of a linear combination of right eigenvectors of $\bar{\boldsymbol{A}}$, with coefficients given by projection onto the left eigenvectors of $\boldsymbol{A}_{p-k}(ik_m)$ [see Eqs. (11) and (12)], is geometrically not consistent. Indeed, for the expression of $\boldsymbol{b}$ given in Eq. (11) one should have $\hat{b}_m = \boldsymbol{b}^T(ik_m)\boldsymbol{y}^{(m)}$, with $\boldsymbol{z}^{(n)^T}\boldsymbol{y}^{(m)} = \delta_{nm}$ (for δ_{nm} denoting the Kronecker delta), whereas in Eq. (12) $\boldsymbol{y}^{(m)}$ is replaced by $\hat{\boldsymbol{y}}^{(m)}$, which yields $\boldsymbol{z}^{(n)^T}\hat{\boldsymbol{y}}^{(m)} \neq \delta_{nm}$. However, note that from the aeroelastic point of view $\hat{\boldsymbol{y}}^{(m)}$ is the most accurate left eigenvector corresponding to $\boldsymbol{z}^{(m)}$. Finally, fixing the frequency at which the projection of $\boldsymbol{b}$ onto $\hat{\boldsymbol{y}}^{(m)}$ is calculated is an additional arbitrary element in the definition of vector $\bar{\boldsymbol{b}}$ in Eqs. (11) and (12).

Remarks on the Analytic Continuation of $\boldsymbol{Q}$

For the sake of the discussion of the numerical results that will be presented, some remarks concerning the approximations introduced by the $p-k$ method and, therefore, affecting the results from the p–transform method, are introduced. These arise in the expression applied for the continuation of matrix $\boldsymbol{Q}$ over the p plane, from its knowledge on the imaginary axis. Observing that the analytic continuation of the aerodynamic matrix is given by (theory of analytic functions)

$$\boldsymbol{Q}(p) = \boldsymbol{Q}(ik) + \left.\frac{\partial \boldsymbol{Q}(p)}{\partial g}\right|_{g=0} g + \mathcal{O}(g^2) \tag{13}$$

the following items can be pointed out (see also Ref. 25):

1) In the original formulation of the $p-k$ method,[27,28] where the following approximation is applied

$$\boldsymbol{Q}(p) \approx \boldsymbol{Q}(ik) \tag{14}$$

unsteady aerodynamic loads, at a given point of the p plane, are evaluated with a truncation error of the order of g.

2) In the modified $p-k$ method of Ref. 24, matrix $\boldsymbol{Q}$ is approximated using the expression in Eq. (8) that, for $\boldsymbol{Q} = \boldsymbol{Q}_R + i\boldsymbol{Q}_I$ and $p = g + ik$, can be recast as

$$\boldsymbol{Q}(p) \approx \boldsymbol{Q}(ik) + \frac{\boldsymbol{Q}_I(ik)}{k} g \tag{15}$$

From the theory of analytic functions, one obtains (see also Ref. 25)

$$\frac{\boldsymbol{Q}_I(ik)}{k} = \left.\frac{\partial \boldsymbol{Q}(p)}{\partial g}\right|_{g=0} - \left.\frac{\partial^2 \boldsymbol{Q}(ik)}{\partial (ik)^2}\right|_{k=0} ik + \mathcal{O}(k^2)$$

and, therefore [see Eq. (13)], if $k = 0$ and/or $\boldsymbol{Q}(ik)$ is a linear function in k, the approximation of Eq. (15) yields a truncation error of the order of g^2; otherwise, it has the same accuracy as the simple approximation of Eq. (14) (i.e., it is affected by a truncation error of the order of g).

3) From the properties of analytic functions, one has

$$\left.\frac{\partial \boldsymbol{Q}(p)}{\partial g}\right|_{g=0} = \left.\frac{\partial \boldsymbol{Q}(p)}{\partial (ik)}\right|_{g=0} = \frac{\partial \boldsymbol{Q}(ik)}{\partial (ik)}$$

and then, Eq. (13) yields

$$\boldsymbol{Q}(p) \approx \boldsymbol{Q}(ik) + \frac{\partial \boldsymbol{Q}(ik)}{\partial (ik)} g \tag{16}$$

which is a g second-order-error approximation of matrix $\boldsymbol{Q}$, based on its knowledge only along the imaginary axis. The approximation in Eq. (16) is the base of the g method,[25] which is an extension of the $p-k$ algorithm and its modified versions.

Therefore, following the same procedure outlined in this section, but starting from aeroelastic eigensolutions based on the g method, a novel g–transform method could be introduced as an enhancement of the p–transform method, in terms of better accuracy in the description of aerodynamic damping.

Aeroelastic ROM from Finite-State Aerodynamics

In this section we present a second approach for the identification of a linear aeroelastic ROM for stability and gust-response analyses, which is based on the approximation of the p-dependent aerodynamic matrices $\boldsymbol{Q}$ and $\boldsymbol{g}$ by the matrix-fraction expression discussed in Ref. 12. Starting from data of $\boldsymbol{Q}$ and $\boldsymbol{g}$ on the imaginary axis, this RMA model yields a description of aerodynamic forces in terms of a finite number of state variables (see later). Coupling such approximated aerodynamic operator with the structural operator, one obtains a ROM for the aeroelastic system that provides a standard eigenproblem and a time-domain state-space format for the gust-response analysis.

Approximation of the Gust/Displacement Aerodynamic Matrix

Herein, the matrix-fraction approximation technique is applied to the global aerodynamic matrix that relates structural Lagrangian coordinates and gust velocity to unsteady aerodynamic forces. Specifically, for a given M_m we consider the following $[M_m \times (M_m+1)]$ global gust/displacement aerodynamic matrix

$$\bar{\boldsymbol{Q}}(p) = [\boldsymbol{g}(p)\,|\,\boldsymbol{Q}(p)] \tag{17}$$

that is, such that

$$\tilde{\boldsymbol{f}}_A(p) = q_D \bar{\boldsymbol{Q}}(p) \begin{Bmatrix} \tilde{w}_g \\ \tilde{\boldsymbol{q}} \end{Bmatrix} \tag{18}$$

The first step in the procedure for the approximation of $\bar{\boldsymbol{Q}}$ starts from the examination of the asymptotic behavior of forces, as the frequency tends to infinity. The derivation of aerodynamic forces caused by elastic displacements involves one time derivative in the expression relating structural Lagrangian coordinates to boundary conditions (normalwash), and a second time derivative appears in the Bernoulli theorem relating velocity potential to pressure. Furthermore, the analysis of the relationship between normalwash and velocity potential shows that it tends to a limit value as the frequency tends to infinity (for instance, see the Theodorsen lift-deficiency function[29] for oscillating airfoils). These observations demonstrate that, whatever the model used for the prediction of frequency-domain aerodynamic forces, the asymptotic behavior of the transfer functions relating structural Lagrangian coordinates to them is quadratic. However, when transfer functions between gust velocity and aerodynamic forces are considered only one time derivative is present (that from Bernoulli's theorem), and, therefore, their frequency asymptotic behavior is linear.

Extending to forces induced by gust and elastic displacements the formulation introduced in Ref. 12 for displacement-induced forces, we assume the following form for the matrix-fraction approximation:

$$\bar{\boldsymbol{Q}}(p) \approx \hat{\boldsymbol{Q}}(p) = p^2 \hat{\boldsymbol{A}}_2 + p\,\hat{\boldsymbol{A}}_1 + \hat{\boldsymbol{A}}_0 + \left[\sum_{n=0}^{N} \boldsymbol{D}_n p^n\right]^{-1} \left[\sum_{n=0}^{N-1} \boldsymbol{R}_n p^n\right] \tag{19}$$

The matrices $\hat{\boldsymbol{A}}_n$, $\boldsymbol{D}_n$, and $\boldsymbol{R}_n$ are real and fully populated, except for $\boldsymbol{D}_N$, which is chosen to be a unit matrix and $\hat{\boldsymbol{A}}_2$ that has the first column equal to zero because of the frequency asymptotic behavior of the aerodynamic loads caused by gust. They are determined by a least-square approximation technique along the imaginary axis. Specifically, the satisfaction of the following condition is required:

$$\epsilon^2 = \sum_j w_j\, \boldsymbol{Tr}\left[\boldsymbol{W}^*(p_j)\boldsymbol{W}(p_j)\right]\Big|_{p_j = ik_j} = \min \tag{20}$$

where w_j denote a suitable set of weights, k_j are the discrete set of reduced frequencies where aerodynamic-matrix data are available, and

$$\boldsymbol{W}(p) = \left[\sum_{n=0}^{N} \boldsymbol{D}_n p^n\right]\left[p^2\hat{\boldsymbol{A}}_2 + p\hat{\boldsymbol{A}}_1 + \hat{\boldsymbol{A}}_0 - \bar{\boldsymbol{Q}}(p)\right] + \sum_{n=0}^{N-1} \boldsymbol{R}_n p^n$$

is proportional to the error $(\hat{\boldsymbol{Q}} - \bar{\boldsymbol{Q}})$.

Next, in order to use the matrix-fraction approximation of matrix $\bar{\boldsymbol{Q}}$ for determining the time-domain relationship between the variables $\boldsymbol{q}$ and w_g, and the aerodynamic forces $\boldsymbol{f}_A$, Eq. (19) is recast in the following form:

$$\hat{\boldsymbol{Q}}(p) = p^2\hat{\boldsymbol{A}}_2 + p\hat{\boldsymbol{A}}_1 + \hat{\boldsymbol{A}}_0 + \hat{\boldsymbol{C}}\,[p\boldsymbol{I} - \hat{\boldsymbol{G}}]^{-1}\hat{\boldsymbol{B}} \tag{21}$$

where[12]

$$\hat{\boldsymbol{C}} = [\boldsymbol{I},\quad \boldsymbol{0},\quad \cdots\quad \boldsymbol{0},\quad \boldsymbol{0}], \qquad \hat{\boldsymbol{B}} = \begin{bmatrix} \boldsymbol{R}_{M-1} \\ \boldsymbol{R}_{M-2} \\ \vdots \\ \boldsymbol{R}_1 \\ \boldsymbol{R}_0 \end{bmatrix}$$

and

$$\hat{\boldsymbol{G}} = \begin{bmatrix} -\boldsymbol{D}_{M-1} & \boldsymbol{I} & \boldsymbol{0} & \dots & \boldsymbol{0} \\ -\boldsymbol{D}_{M-2} & \boldsymbol{0} & \boldsymbol{I} & \dots & \boldsymbol{0} \\ \vdots & \vdots & & & \vdots \\ -\boldsymbol{D}_1 & \boldsymbol{0} & \boldsymbol{0} & \dots & \boldsymbol{I} \\ -\boldsymbol{D}_0 & \boldsymbol{0} & \boldsymbol{0} & \boldsymbol{0} & \boldsymbol{0} \end{bmatrix}$$

The accuracy of the approximation depends upon the number N of matrices used in the matrix-fraction term in Eq. (19). The appropriate value of N depends, for a prescribed accuracy, upon the shape of the functions to be approximated and on the dimensions of $\bar{\boldsymbol{Q}}$. In our case, despite the fact that these functions have a regular behavior in the frequency domain, for a high number of structural Lagrangian coordinates a satisfactory accuracy of the approximation requires a value of N that generates a high number of poles [eigenvalues of the matrix $\hat{\boldsymbol{G}}$ in Eq. (21)]. This, in turn, might induce the presence of unstable poles (i.e., poles having real part greater than zero); these are spurious poles that are introduced by the interpolation procedure and do not describe the physical behavior of the aerodynamic phenomena. To overcome this problem, an iterative procedure is adopted.[12] This consists of 1) diagonalization (or block diagonalization) of $\hat{\boldsymbol{G}}$, 2) truncation of the unstable poles (the matrix $\hat{\boldsymbol{G}}$ is modified into a smaller matrix $\boldsymbol{G}$), and 3) application of an optimal fit iterative procedure to determine new matrices $\boldsymbol{A}_2$, $\boldsymbol{A}_1$, $\boldsymbol{A}_0$, $\boldsymbol{B}$, and $\boldsymbol{C}$ that replace, respectively, $\hat{\boldsymbol{A}}_2$, $\hat{\boldsymbol{A}}_1$, $\hat{\boldsymbol{A}}_0$, $\hat{\boldsymbol{B}}$, and $\hat{\boldsymbol{C}}$. The matrix $\boldsymbol{G}$ remains unchanged throughout the iteration.

Hence, the matrix-fraction approximation ensuring a good and stable fit of $\bar{\boldsymbol{Q}}(p)$ has the final form:

$$\hat{\boldsymbol{Q}}(p) = p^2\boldsymbol{A}_2 + p\boldsymbol{A}_1 + \boldsymbol{A}_0 + \boldsymbol{C}[p\boldsymbol{I} - \boldsymbol{G}]^{-1}\boldsymbol{B} \tag{22}$$

It is worth pointing out that the well-known finite–state reduction method introduced by Karpel[6,9] directly starts from an expression of the type of that in Eq. (22). This means that the dimensions of matrix $\boldsymbol{G}$ can be set arbitrarily in dependence of the number of additional states that are presumed to be necessary, but the drawback is that the identification of the matrices in Eq. (22) would require the iterative solution of a nonlinear algebraic problem. In the approach used here the coefficients of the starting expression in Eq. (19) are determined by solving the linear algebraic equation resulting from the least-square technique applied to Eq. (20). No iterations are needed for determining the matrices in Eqs. (19) and (21), but the number of the additional states introduced is forced to be N times the number of the generalized forces described by the aerodynamic matrix.

(In Ref. 12 an alternate formulation is presented; using that, the number of the additional states is forced to be N times the number of the aerodynamic-matrix input variables). If this number overestimates the number of the additional states required by the problem, unstable poles arise, and, as just mentioned, also in this case an iterative procedure has to be applied for their elimination. Thus, Karpel's method and the method applied here are very similar. The main difference is that in Karpel's method the number of additional states is chosen a priori, whereas in the method applied here it is given by a self-fitting procedure.

Analytic Continuation of $\hat{\boldsymbol{Q}}$

As already mentioned in this section, the coefficients of the rational-matrix approximation of $\bar{\boldsymbol{Q}}$ have been determined through a least-square-approximation approach applied along the imaginary axis. This procedure is applicable because of the properties of the analytic functions. Indeed, observing that for an arbitrary analytic function $f(p)$ we have $\partial f(p)10g = \partial f(p)/\partial(ik)$, it is possible to show that if the expression of the analytic function is known in terms of the variable ik (i.e., along the imaginary axis), then the same expression with ik replaced by p describes the function over its domain of analyticity in the p plane. In our problem this means that if $\hat{\boldsymbol{Q}} \approx \bar{\boldsymbol{Q}}$ [see Eq. (19)] along the imaginary axis, then this is true over their domain of analyticity, with the same accuracy provided by the least-square procedure along the imaginary axis.

ROM for Aeroelastic Gust Response

For the sake of deriving the aeroelastic ROM of the gust-response problem, matrices $\boldsymbol{A}_k$ and $\boldsymbol{B}$ in Eq. (22) are partitioned in the following way:

$$\boldsymbol{A}_k = [\boldsymbol{a}_k \,|\, \check{\boldsymbol{A}}_k], \qquad \boldsymbol{B} = [\check{\boldsymbol{b}} \,|\, \check{\boldsymbol{B}}]$$

where the $\boldsymbol{a}_k$ are of dimensions $[M_m \times 1]$ with $\boldsymbol{a}_2 = \boldsymbol{0}$ caused by the asymptotic behavior of gust loads and matrices $\check{\boldsymbol{A}}_k$ are of dimensions $[M_m \times M_m]$. In addition, $\check{\boldsymbol{b}}$ is of dimensions $[M_p \times 1]$, and $\check{\boldsymbol{B}}$ is of dimensions $[M_p \times M_m]$, with M_p denoting the number of eigenvalues of matrix $\boldsymbol{G}$. Then, combining Eq. (22) with Eq. (18) and replacing $\bar{\boldsymbol{Q}}$ with $\hat{\boldsymbol{Q}}$, transformation into time domain yields

$$\boldsymbol{f}_A(\tau)/q_D = \check{\boldsymbol{A}}_2\ddot{\boldsymbol{q}} + \check{\boldsymbol{A}}_1\dot{\boldsymbol{q}} + \check{\boldsymbol{A}}_0\boldsymbol{q} + \boldsymbol{a}_1\dot{w}_g + \boldsymbol{a}_0 w_g + \boldsymbol{C}\boldsymbol{r} \tag{23}$$

with

$$\dot{\boldsymbol{r}} = \boldsymbol{G}\boldsymbol{r} + \check{\boldsymbol{B}}\boldsymbol{q} + \check{\boldsymbol{b}}w_g \tag{24}$$

where $(\ddot{\ }) = \mathrm{d}^2/\mathrm{d}\tau^2$ and $(\dot{\ }) = \mathrm{d}/\mathrm{d}\tau$.

The additional states, $\boldsymbol{r}$, generated by the matrix-fraction approximation of $\bar{\boldsymbol{Q}}$ are a consequence of its transcendental nature, that is, of flow-memory effects caused by compressibility and/or vorticity convected in the wake. Indeed, prior wing dynamics influences current aerodynamic field both as a result of the delays in propagation of perturbations in compressible flows and as a result of the presence of vortices (in the wake) previously released at the trailing edge. Therefore, instead of approximating separately $\boldsymbol{Q}$ and $\boldsymbol{g}$ we have approximated the global matrix, $\bar{\boldsymbol{Q}}$, because in the former case we would have obtained a set of additional states from the approximation of $\boldsymbol{Q}$ and a different set of additional states from the approximation of $\boldsymbol{g}$. This would have been in contrast with the common origin of such additional states. (Similar considerations have already been discussed in Ref. 30 and used in the applications to wing-tail configurations presented in Refs. 14 and 31).

Next, combining Eqs. (23) and (24) with Eq. (1) yields the following state-space format for the aeroelastic gust response of a wing based on the RMA formulation:

$$\dot{\boldsymbol{x}} = \boldsymbol{A}_{\mathrm{RMA}}\boldsymbol{x} + \boldsymbol{h}_1\dot{w}_g + \boldsymbol{h}_0 w_g \tag{25}$$

with $\boldsymbol{x}^T = \{\boldsymbol{q}^T\,\dot{\boldsymbol{q}}^T\,\boldsymbol{r}^T\}$ and for $\boldsymbol{M} = (\boldsymbol{I} - q_D\check{\boldsymbol{A}}_2)$

$$\boldsymbol{A}_{\mathrm{RMA}} = \begin{bmatrix} \boldsymbol{0} & \boldsymbol{I} & \boldsymbol{0} \\ \boldsymbol{M}^{-1}\left(q_D\check{\boldsymbol{A}}_0 - \Omega^2\right) & q_D\boldsymbol{M}^{-1}\check{\boldsymbol{A}}_1 & q_D\boldsymbol{M}^{-1}\boldsymbol{C} \\ \check{\boldsymbol{B}} & \boldsymbol{0} & \boldsymbol{G} \end{bmatrix} \tag{26}$$

whereas

$$\boldsymbol{h}_1 = \begin{Bmatrix} \boldsymbol{0} \\ q_D\boldsymbol{M}^{-1}\boldsymbol{a}_1 \\ \boldsymbol{0} \end{Bmatrix}, \qquad \boldsymbol{h}_0 = \begin{Bmatrix} \boldsymbol{0} \\ q_D\boldsymbol{M}^{-1}\boldsymbol{a}_0 \\ \check{\boldsymbol{b}} \end{Bmatrix}$$

Finally, the gust-transfer-function matrix that relates gust velocity to the $2M_m$ structural states and the M_p additional states is given by

$$\boldsymbol{H}_{\mathrm{RMA}}(p) = [p\boldsymbol{I} - \boldsymbol{A}_{\mathrm{RMA}}]^{-1}(p\boldsymbol{h}_1 + \boldsymbol{h}_0)$$

with the following corresponding characteristic equation:

$$|p\boldsymbol{I} - \boldsymbol{A}_{\mathrm{RMA}}| = 0$$

Numerical Results

Validation of Finite-State Approximation for Aerodynamics

To validate the finite-state approximation for aerodynamics just outlined, the aerodynamic transfer functions included in the aeroelastic operators of two different wing models are considered.

First, the wing model (WING1) introduced in Ref. 32, consisting of a rectangular unswept wing having half-span length equal to 4.57 m and chord length equal to 1.27 m (see Ref. 32), is analyzed. Using six natural modes of vibration for describing the elastic deformation, the aerodynamic transfer functions have been computed at prescribed points along the imaginary axis of the p plane at $M = 0.55$ and $\rho = 1.23$ kg/m^3, by altering the MSC.NASTRAN code flow in the gust-response solution sequence. This solution is based on the doublet-lattice method approach for potential flows,[26] and for our problem the wing surface has been discretized by 16 chordwise panels and 8 spanwise panels. Figures 1–3 compare the calculated transfer function Q_{12} relating the second Lagrangian coordinate to the first generalized aerodynamic force (data) with its rational-matrix approximation (RMA). Specifically, the rational-matrix approximation shown in Fig. 1 has been obtained using only two poles [$M_p = 2$, for matrices in Eq. (22)], whereas the approximated transfer functions presented in Figs. 2 and 3 have been obtained using, respectively, 5 and 10 poles. These figures demonstrate that, as expected, the accuracy of the approximated transfer functions increases with the number of the poles included in the rational expression and that, furthermore, a very good agreement with the computed values can be achieved. This behavior is shown by all of the aerodynamic transfer functions collected in $\bar{\boldsymbol{Q}}$.

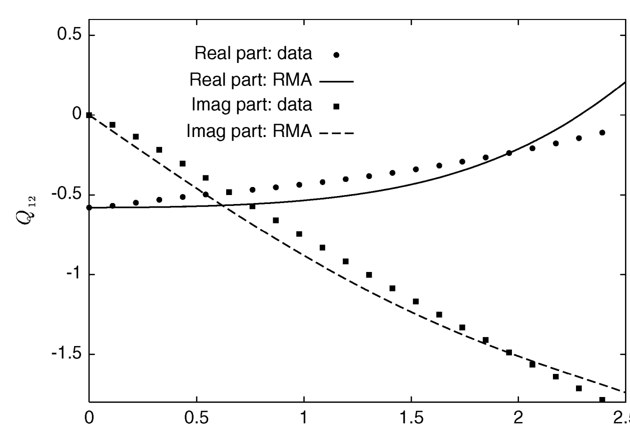

Fig. 1 Aerodynamic transfer function $Q_{12}(k)$ for WING1: two-pole approximation.

Table 1 Glider half-wing geometry

Parameter	Value
Length, m	2.85
Weight, kg	2.244
Root chord, m	0.283
Tip chord, m	0.074
Mean chord, m	0.187
Surface, m^2	1.12
Root thickness/chord	0.045
Tip thickness/chord	0.014
Aspect ratio	14
Control surface length, m	1.46
Control surface chord, m	0.04

Table 2 Glider wing modal analysis

Modes	Natural frequecies, Hz
1st B[a]	3.068
1st in-plane B	14.638
2nd B	15.130
3rd B–T[b]	34.593
1st T	46.275
4th B–T	57.507
5th B–T	69.228
6th B–T	74.589
7th B–T	80.834

[a]B = bending, [b]T = torsion.

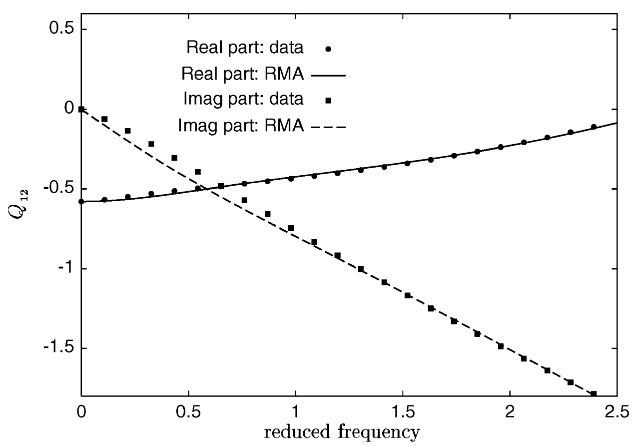

Fig. 2 Aerodynamic transfer function $Q_{12}(k)$ for WING1: five-pole approximation.

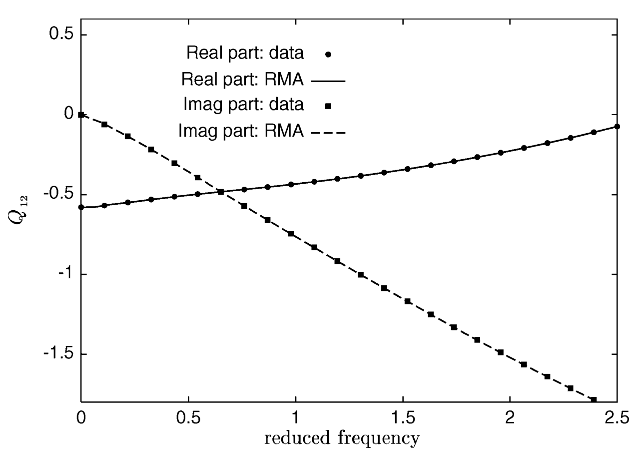

Fig. 3 Aerodynamic transfer function $Q_{12}(k)$ for WING1: 10-pole approximation.

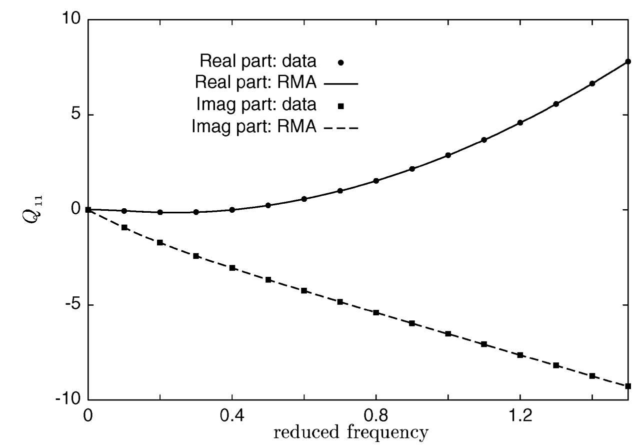

Fig. 4 Aerodynamic transfer function $Q_{11}(k)$ for WING2: 12-pole approximation.

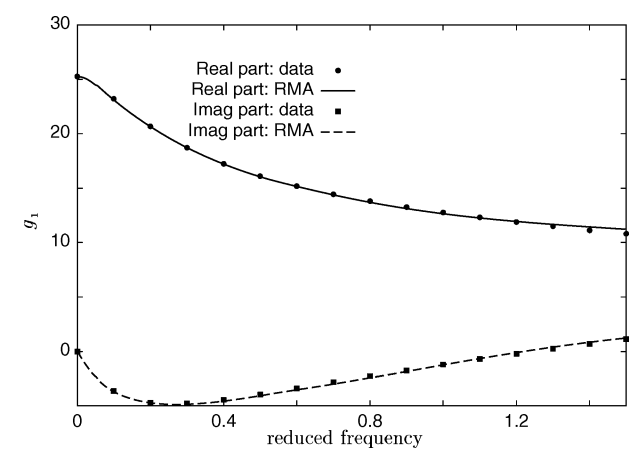

Fig. 5 Gust aerodynamic transfer function $g_1(k)$ for WING2: 12-pole approximation.

A similar analysis has also been performed for a higher-aspect-ratio, highly flexible glider-model composite wing (WING2) that has the geometric characteristics listed in Table 1. This wing has a fiber glass skin and two sandwich spars with carbon-fiber and glass-fiber skin and spruce core. Structural analysis for this wing has been performed using the finite element MSC.NASTRAN code with 1668 quadrilateral elements to model the composite skin and the two composite spars. Results of this numerical dynamic analysis are shown in Table 2 (see also Ref. 33 where a passive control is applied to WING2). Also in this case unsteady aerodynamic loads at given points along the imaginary axis of the p plane (at $M = 0$ and $\rho = 1.23\,\mathrm{kg/m^3}$) have been obtained by using the doublet-lattice method, with 10 chordwise panels and 22 spanwise panels for the discretization of the wing surface. For a number of poles equal to 12, Fig. 4 shows the comparison between calculated (data) and approximated (RMA) aerodynamic transfer function Q_{11}, whereas Fig. 5 shows the comparison between calculated and approximated gust aerodynamic transfer function g_1 (i.e., the first entry of $\boldsymbol{g}$ that relates gust velocity to the first generalized aerodynamic force). The agreement between calculated and approximate curves appears to be very good, both for the aerodynamic loads caused by elastic deformation and for those induced by the gust. (This agreement is shown by all of the transfer functions of $\bar{\boldsymbol{Q}}$.)

Note that throughout the numerical investigation a 1% maximum relative error has been considered as convergence condition of the iterative procedure for the elimination of spurious poles in the RMA approach.

Stability Analysis

Next, we have examined the aeroelastic stability behavior of the two wing models just presented, using both the p–transform method and the aeroelastic ROM obtained from the RMA approach. For all of the results from the p–transform method that will be presented, the approximate system matrix $\bar{\boldsymbol{A}}$ and gust vector $\bar{\boldsymbol{b}}$ [see

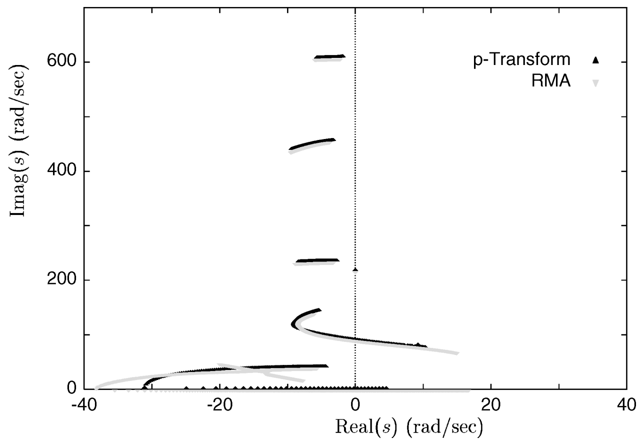

Fig. 6 Aeroelastic root loci of WING1.

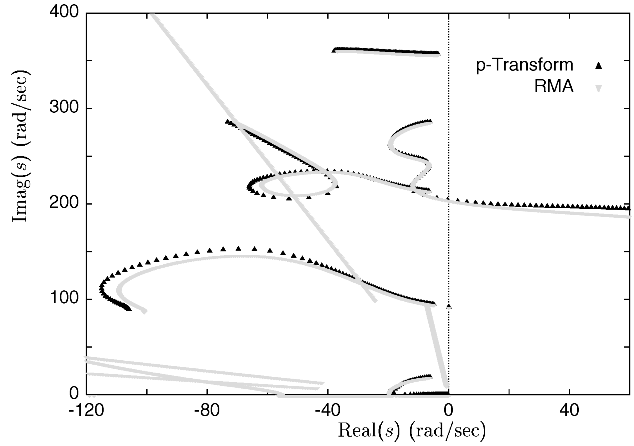

Fig. 7 Aeroelastic root loci of WING2.

Eqs. (10) and (11)] have been obtained through aeroelastic eigenanalyses performed by the modified $p-k$ method available in the MSC.NASTRAN code.

Figure 6 depicts aeroelastic root loci of WING1 in the plane of the dimensional Laplace variable s, given as parametric functions of the flight velocity, comparing results from the two ROMs presented. Because of the different approximation of the aerodynamic loads, these two results appear to be in very good agreement close to the imaginary axis but with some discrepancies where aerodynamic damping is significant. Indeed, as already observed, at each point of the complex plane the approximation of the aerodynamic operator given by the RMA approach is as accurate as that given along the imaginary axis, whereas the accuracy of the aerodynamic operator considered in the p–transform method is reduced moving from the imaginary axis. The error introduced increases quadratically with g if $k=0$ or if $\boldsymbol{Q}(ik)$ is a linear function of k; otherwise, it increases linearly with g. However, the stability margins predicted by the two approaches are almost identical: the RMA approach (with $M_p=10$) predicts flutter at $V_{\mathrm{FL}}=257$ m/s, with $f_{\mathrm{FL}}=14.2$ Hz (where $f=\omega/2\pi$), whereas the p–transform method predicts flutter at $V_{\mathrm{FL}}=255$ m/s with $f_{\mathrm{FL}}=14.3$ Hz. Divergence has also been computed by the RMA at $V_D=288$ m/s and by the p–transform method at $V_D=290$ m/s.

Similar considerations are applicable to the root loci depicted in Fig. 7, which are provided by the aeroelastic analysis of WING2. In this case the flutter velocity computed from the RMA approach (with $M_p=12$) is $V_{\mathrm{FL}}=139.25$ m/s with $f_{\mathrm{FL}}=32.5$ Hz, whereas from the p–transform method we have obtained $V_{\mathrm{FL}}=139.5$ m/s and $f_{\mathrm{FL}}=32.4$ Hz.

Note that in Figs. 6 and 7 some of the roots determined from application of the RMA describe quasi-straight paths, whereas no equivalent roots are given by the p–transform method. These are the roots introduced by the additional aerodynamic states, which, in terms of the reduced complex frequency, p, are very close to the eigenvalues of the matrix $\boldsymbol{G}$ of Eq. (22), and hence vary linearly with the velocity when the dimensional complex frequency, s, is used (as in Figs. 6 and 7). The small difference between aerodynamic-state roots and eigenvalues of $\boldsymbol{G}$ signifies that the coupling between structural states and aerodynamic states given by the matrix $\check{\boldsymbol{B}}$ in the system matrix $\boldsymbol{A}_{\mathrm{RMA}}$ [see Eq. (26)] is weak.

Gust-Response Analysis

Next, we analyze the capability of the p–transform method and of the RMA approach to predict the aeroelastic response to an arbitrary vertical gust. Specifically, we examine the approximate gust-transfer-function (column) matrices $\boldsymbol{H}_{p-t}$ and $\boldsymbol{H}_{\mathrm{RMA}}$ given by the two methods just described, comparing both of them with that computed at discrete points along the imaginary axis of the s plane using the MSC.NASTRAN code.

First, we show the results concerning WING1 for $V=190$ m/s and $M=0.55$. Figure 8 depicts real and imaginary parts of $H_1(f)$ (i.e., the frequency-response function that relates gust velocity, w_g, to the first structural modal amplitude, q_1), whereas Fig. 9 depicts real and imaginary parts of $H_6(f)$ (i.e., the frequency-response function relating w_g to q_6). Observing these figures, it appears that the results from the RMA approach are in excellent agreement with those obtained from the MSC.NASTRAN code, whereas results given by the p–transform approach show significant local discrepancies. As can be deduced from the description of the p–transform method, these discrepancies are caused by both the (possible) poor accuracy of the approximated aeroelastic operator in points of the complex plane far from the aeroelastic eigenvalues used for defining the system matrix $\bar{\boldsymbol{A}}$ and the arbitrary elements that have been introduced in defining the approximate vector $\bar{\boldsymbol{b}}$.

Similar results have been obtained for WING2 at $V=40$ m/s and $M=0$. These are illustrated in Figs. 10 and 11, from which it is apparent that the p–transform approach might yield inaccurate results at very low frequencies (in this case those below the first aeroelastic eigenvalue of WING2), where even very simple aeroelastic models based on quasi-steady aerodynamics are satisfactorily accurate.

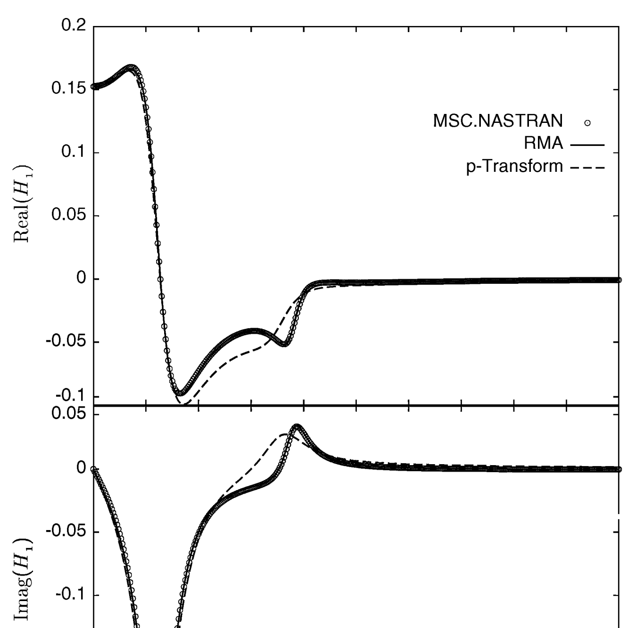

Fig. 8 WING1 frequency-response function $\boldsymbol{H_1(f)}$.

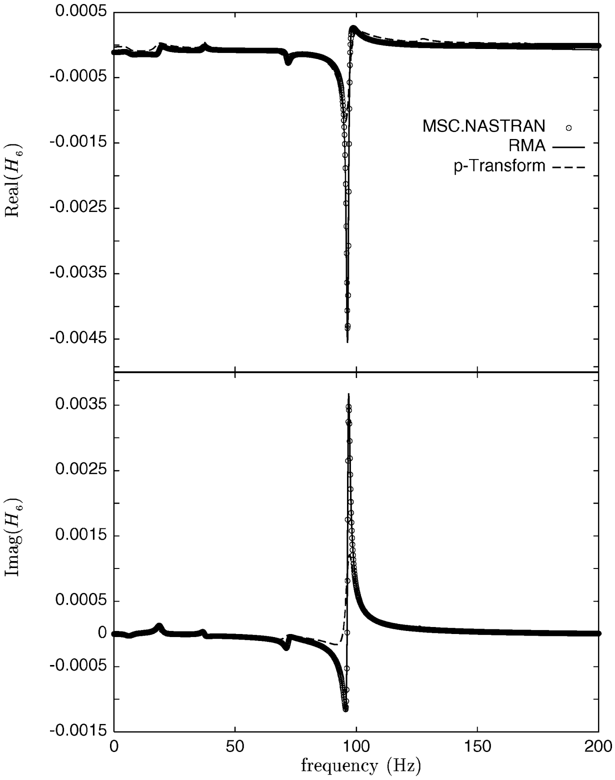

Fig. 9 WING1 frequency-response function $H_6(f)$.

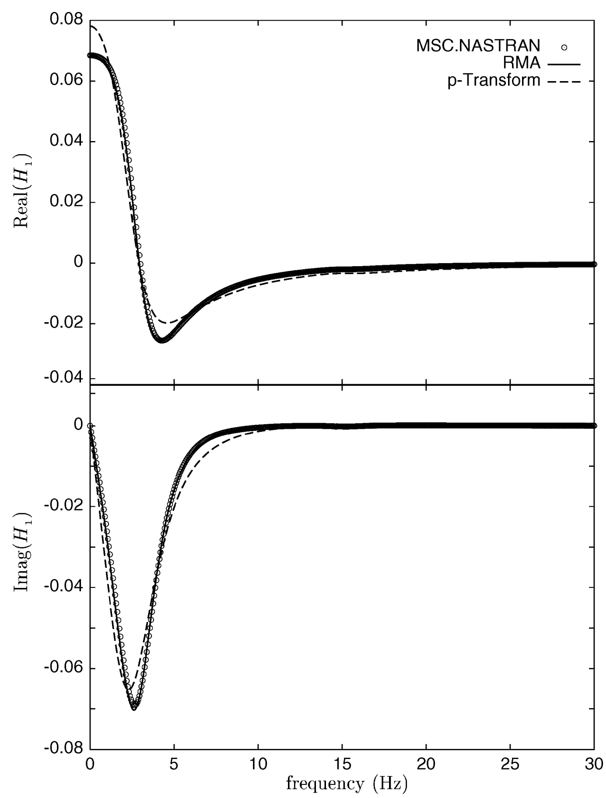

Fig. 10 WING2 frequency-response function $H_1(f)$.

These results demonstrate that for the gust-response analysis the p–transform method might show significant inaccuracies that derive from the criteria of approximation through which $\bar{A}$ and $\bar{b}$ are determined. On the other hand, the results obtained by applying the RMA approach are very accurate. A drawback of this method is in the introduction of additional states that might cause an increase in the computational cost and make it less appealing for preliminary design and control applications. Thus, an alternate ROM, merging the advantages of the two methods, is discussed in the next paragraph.

Gust-Response ROM from p–Transform/RMA Combination

From the stability results just presented, it is apparent that without introducing additional states the p–transform method is capable of predicting with satisfactory accuracy the eigensolution of a wing aeroelastic problem. In addition, the gust-response results have

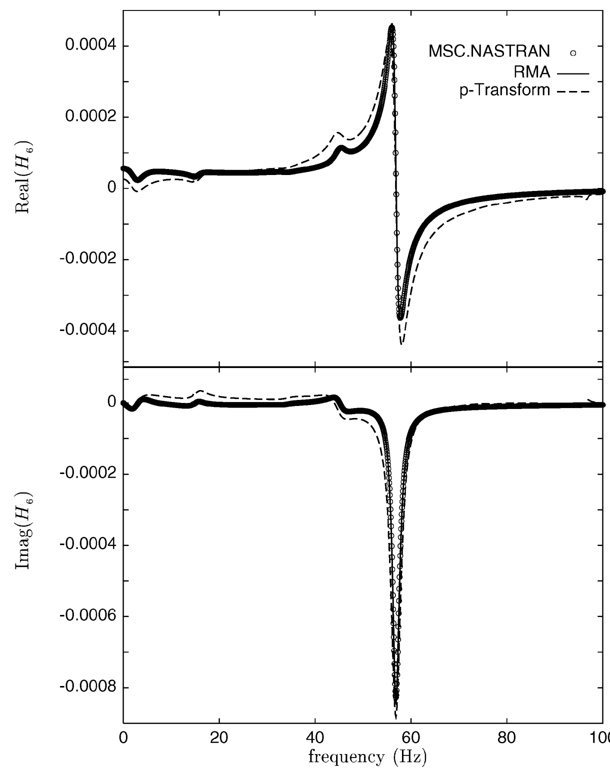

Fig. 11 WING2 frequency-response function $H_6(f)$.

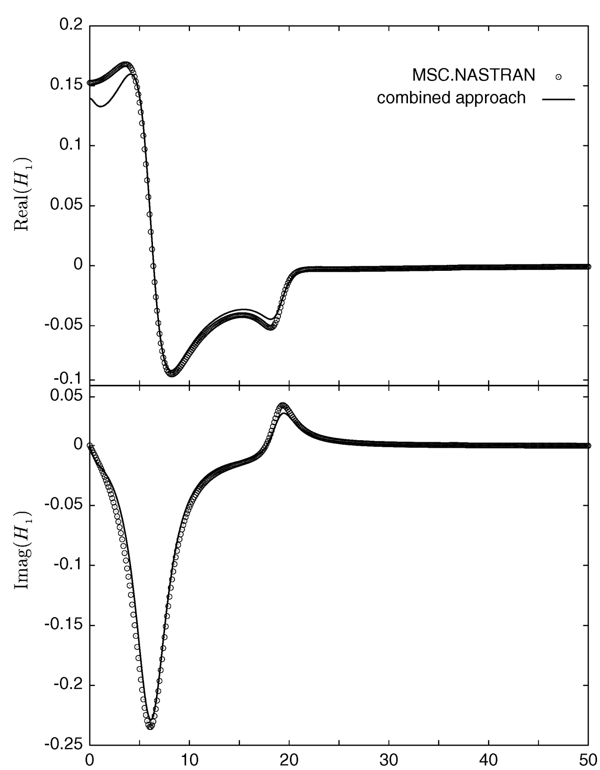

Fig. 12 WING1 frequency-response function $H_1(f)$: combined approach with a six-pole RMA.

demonstrated the need for applying the RMA approach for an accurate gust-response analysis. Starting from these observations, an alternate gust-response ROM is presented. It consists of modeling the aeroelastic operator through the matrix $\bar{A}$ of the p–transform method (not requiring introduction of additional states), combined with gust-forcing terms expressed by the RMA approach. Theoretically, the number of poles required by the RMA approach for modeling only vector $\boldsymbol{g}$ is equal to that required for modeling the

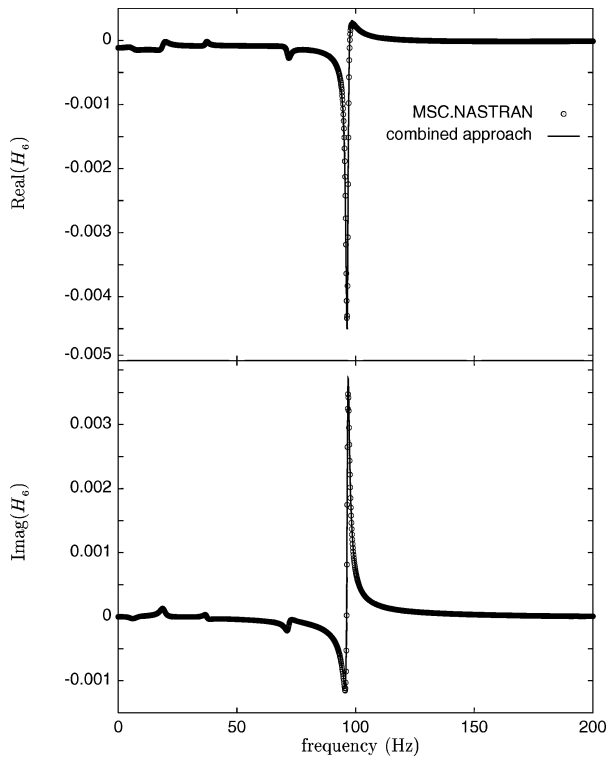

Fig. 13 WING1 frequency-response function $H_6(f)$: combined approach with a six-pole RMA.

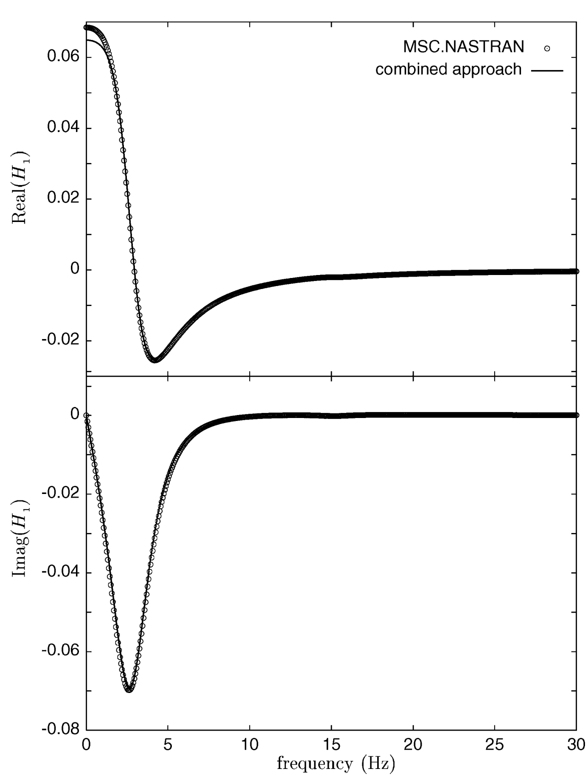

Fig. 14 WING2 frequency-response function $H_1(f)$: combined approach with a seven-pole RMA.

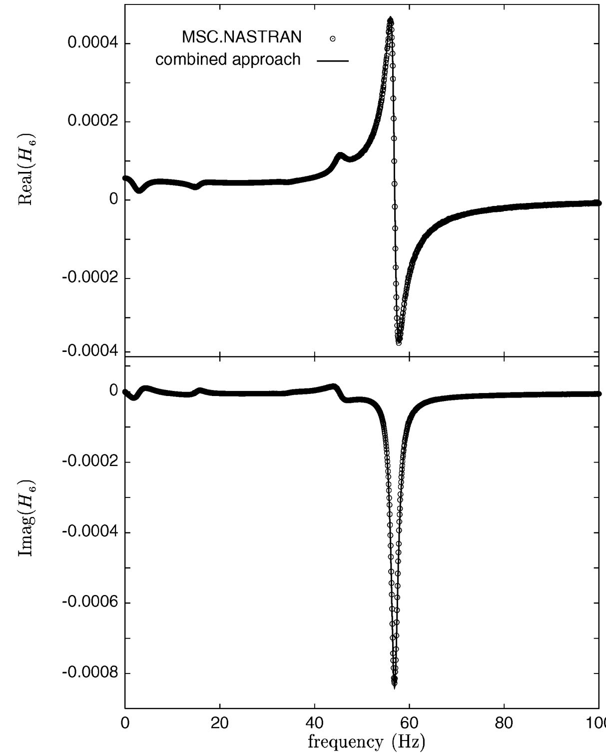

Fig. 15 WING2 frequency-response function $H_6(f)$: combined approach with a seven-pole RMA.

global aerodynamic matrix, $\bar{\boldsymbol{Q}}$. However, the advantage in using the combined approach is that, from the numerical point of view, this number can be smaller (with a limited loss of accuracy) because of the reduction of the number of transfer functions to be approximated (reduction of the spanned functional space).

For WING1 configuration Figs. 12 and 13 depict the comparison between frequency-response functions computed by the MSC.NASTRAN code and those obtained by the combined approach with $M_p = 6$ for the approximation of vector $\boldsymbol{g}$. Comparing these results with those illustrated in Figs. 8 and 9, it is apparent that this approach has the capability of predicting gust responses with an accuracy similar to that given by the RMA approach, but using a lower number of additional states. ($M_p = 10$ has been used for the results in Figs. 8 and 9.)

This capability is also confirmed by the investigation of the gust response of WING2. Indeed, using $M_p = 7$ for the approximation of $\boldsymbol{g}$ we have obtained the results presented in Figs. 14 and 15 that show a level of accuracy similar to that obtained by the RMA method with the inclusion of 12 poles (see Figs. 10 and 11).

Conclusions

Three different linear aeroelastic reduced-order models (ROMs), addressed to the analysis of flutter and gust response of a flexible wing, have been outlined and compared. First, the p–transform method has been considered, which provides directly a ROM for the aeroelastic system via knowledge of the aeroelastic eigenvalues (and corresponding eigenvectors) closest to the structural eigenvalues. Then, a finite-state-aerodynamics approach has been considered based on the rational approximation of the transfer functions relating aerodynamic forces to wing elastic displacements and gust velocity. From this, it is possible to derive a ROM for the aeroelastic operator, enriched by the presence of some aerodynamic states added to the structural states.

The p–transform method yields an aeroelastic ROM expressed only in terms of the structural states, but the numerical investigation has demonstrated that it represents with good accuracy only the dynamics of those modal degrees of freedom which are moderately damped. When the wing is forced by a gust, the p–transform method predicts the corresponding frequency-response functions with local inaccuracies. Therefore, this method does not seem to be very reliable for providing an aeroelastic ROM to be applied, for instance, in the design of control devices for gust-load alleviation.

As shown by numerical results, the aeroelastic ROM obtained from the RMA approach is capable of predicting with very good accuracy both the eigensolution of the aeroelastic operator and the frequency-response functions to gusts, but it deals with a higher number of states because of the introduction of the aerodynamic states. This can considerably increase the complexity of the mathematical model to manage with in preliminary design and in control processes.

Finally, an alternate ROM for gust-response problems has been introduced that couples the aeroelastic matrix given by the *p*–transform method with the gust-force vector approximated through the RMA approach. This combined approach evaluates the eigen-solution of the aeroelastic operator with the same accuracy of the *p*–transform method, but numerical investigations have demonstrated that it predicts frequency-response functions to gusts with an accuracy comparable to that of the RMA approach with a reduced number of additional states. Hence, the combined *p*–transform/RMA approach provides a simpler aeroelastic ROM that can be conveniently applied for preliminary design and control purposes.

References

[1]Dowell, E. H., Hall, K. C., and Romanowski, M. C., "Eigenmode Analysis in Unsteady Aerodynamics: Reduced Order Models," *Applied Mechanics Review*, Vol. 50, No. 6, 1997, pp. 371–386.

[2]Jones, R. T., "The Unsteady Lift of a Wing of Finite Aspect Ratio," NACA Rept. 681, June 1940.

[3]Vepa, R., "On the Use of Padé Approximants to Represent Unsteady Aerodynamic Loads for Arbitrarily Small Motions of Wings," AIAA Paper 76-17, Jan. 1976.

[4]Roger, K. L., "Airplane Math Modeling Methods for Active Control Design," AGARD-CP-228, Aug. 1977, pp. 4-1–4-10.

[5]Edwards, J. W., Ashley, H., and Breakwell, J. V., "Unsteady Aerodynamic Modeling for Arbitrary Motions," *AIAA Journal*, Vol. 17, No. 4, 1979, pp. 365–374.

[6]Karpel, M., "Design for the Active Flutter Suppression and Gust Alleviation Using State-Space Aeroelastic Modeling," *Journal of Aircraft*, Vol. 19, No. 3, 1982, pp. 221–227.

[7]Mukhopadhyay, V., Newson, J. R., and Abel, I., "Reduced-Order Optimal Feedback Control Law Synthesis for Flutter Suppression," *Journal of Guidance, Control, and Dynamics*, Vol. 5, No. 4, 1982, pp. 389–395.

[8]Liebst, B. S., Garrard, W. L., and Adams, W. M., "Design of an Active Flutter Suppression System," *Journal of Guidance, Control, and Dynamics*, Vol. 9, No. 1, 1986, pp. 64–71.

[9]Karpel, M., "Time-Domain Aeroservoelastic Modeling Using Weighted Unsteady Aerodynamic Forces," *Journal of Guidance, Control and Dynamics*, Vol. 13, No. 1, 1990, pp. 30–37.

[10]Karpel, M., "Reduced-Order Aeroelastic Models via Dynamic Residualization," *Journal of Aircraft*, Vol. 27, No. 5, 1990, pp. 449–455.

[11]Hoadley, S. T., and Karpel, M., "Application of Aeroservoelastic Modeling Using Minimum-State Unsteady Aerodynamic Approximations," *Journal of Guidance, Control, and Dynamics*, Vol. 14, No. 6, 1991, pp. 1267–1276.

[12]Morino, L., Mastroddi, F., De Troia, R., Ghiringhelli, G. L., and Mantegazza, P., "Matrix Fraction Approach for Finite-State Aerodynamic Modeling," *AIAA Journal*, Vol. 33. No. 4, 1995, pp. 703–711.

[13]Zang, T. A., and Green, L. L., "Multidisciplinary Design Optimization Techniques: Implications and Opportunities for Fluid Dynamics Research," AIAA Paper 99-3798, June–July 1999.

[14]Gennaretti, M., and Ponzi, C., "Finite-State Aerodynamic Modelling for Gust Load Alleviation of Wing-Tail Configurations," *The Aeronautical Journal*, Vol. 103, No. 1021, 1999, pp. 147–158.

[15]Gennaretti, M., and Lisandrin, P., "Flap-Lag Rotor Dynamics and Aeroelastic Stability Using Finite-State Aerodynamics," *Proceedings of the 24th European Rotorcraft Forum*, AAAF, Marseilles, France, 1998, pp. DY.01.1–DY.01.11.

[16]Raveh, D., Levy, Y., and Karpel, M., "Efficient Aeroelastic Analysis Using Computational Unsteady Aerodynamics," *Journal of Aircraft*, Vol. 38, No. 3, 2001, pp. 547–556.

[17]Raveh, D., "Reduced-Order Models for Nonlinear Unsteady Aerodynamics," *AIAA Journal*, Vol. 39, No. 8, 2001, pp. 1417–1429.

[18]Silva, W. A., "Application of Nonlinear System Theory to Transonic Unsteady Aerodynamic Responses," *Journal of Aircraft*, Vol. 30, No. 5, 1993, pp. 660–668.

[19]Silva, W. A., "Reduced Order Models Based in Linear and Nonlinear Aerodynamics Impulse Response," *Proceedings of the CEAS/AIAA/ICASE/NASA Langley International Forum on Aeroelasticity and Structural Dynamics*, NACA/CP-1999-209136/PT1, 1999, pp. 369–379.

[20]Silva, W. A., and Bartels, R. E., "Development of Reduced-Order Models for Aeroelastic Analysis and Flutter Prediction Using the CFL3Dv6.0 Code," AIAA Paper 2002-1596, April 2002.

[21]Hall, K. C., Thomas, J. P., and Dowell, E. H., "Proper Orthogonal Decomposition Technique for Transonic Unsteady Aerodynamic Flows," *AIAA Journal*, Vol. 38, No. 10, 2000, pp. 1853–1862.

[22]Beran, P. S., and Silva, W. A., "Reduced-Order Modeling: New Approaches for Computational Physics," AIAA Paper 2001-0853, Jan. 2001.

[23]Dykman, J. R., and Rodden, W. P., "An Application of the P–Transform Method for Transient Meneuvering Analysis," *Proceedings of the CEAS/AIAA/ICASE/NASA Langley International Forum on Aeroelasticity and Structural Dynamics*, NACA/CP-1999-209136/PT1, 1999, pp. 425–432.

[24]Rodden, W. P., Harder, R. L., and Bellinger, E. D., "Aeroelastic Addition to NASTRAN," NASA CR-3094, March 1979.

[25]Chen, P. C., "A Damping Perturbation Method for Flutter Solution: The g-Method," *AIAA Journal*, Vol. 38, No. 9, 2000, pp. 1519–1524.

[26]Giesing, J. P., Kalman, T. P., and Rodden, W. P., "Subsonic Unsteady Aerodynamics for General Configuration, Part I. Direct Application of the Nonplanar Double-Lattice Method," USAF, Flight Dynamics Lab., Rept. AFFDL-TR-71-5, Vol. 1, Nov. 1971.

[27]Irwin, C. A., and Guyett, P. R., "The Subcritical Response and Flutter of a Swept Wing Model," Royal Aircraft Establishment, Rept. 65186, Farnborough, England, U.K., Aug. 1965.

[28]Hassig, H. J., "An Approximate True Damping Solution of the Flutter Equation by Determinant Iteration," *Journal of Aircraft*, Vol. 8, No. 11, 1971, pp. 885–889.

[29]Theodorsen, T., "General Theory of Aerodynamic Instability and the Mechanism of Flutter," NACA Report 496, 1935.

[30]Pasinetti, G., and Mantegazza, P., "Single Finite States Modeling of Aerodynamic Forces Related to Structural Motions and Gusts," *AIAA Journal*, Vol. 37, No. 5, 1999, pp. 604–612.

[31]De Troia, R., Gennaretti, M., Morino, L., Mastroddi, F., and Pecora, M., "Gust Response of Wing-Tail Configurations," *Proceedings of the CEAS International Forum on Aeroelasticity and Structural Dynamics*, Royal Aeronautical Society, London, UK, 1995, pp. 64.1–64.8.

[32]Rudisill, C. S., and Bhatia, K. G., "Optimization of Complex Structures to Satisfy Flutter Requirements," *AIAA Journal*, Vol. 9, No. 8, 1971, pp. 1487–1491.

[33]Agneni, A., Mastroddi, F., and Polli, G. M., "Modeling of Piezoelectric Patches in Elastic and Aeroelastic Vibrations," *Computer and Structures*, Vol. 81, No. 2, 2003, pp. 91–105.